Pis'ma v ZhETF, vol. 82, iss. 4, pp. 243 – 246

Phase Transition with Suppression of Magnetism in $BiFeO_3$ at High Pressure

A. G. Gavriliuk[+*∇], *V. V. Struzhkin*[+], *I. S. Lyubutin*[*1)], *M. Y. Hu*[□], *H. K. Mao*[+]

[+] *Geophysical Laboratory, Carnegie Institution of Washington, Washington DC 20015, USA*

[*] *Institute of Crystallography RAS, 119333 Moscow, Russia*

[∇] *Institute for High Pressure Physics RAS, 142190 Troitsk, Moscow reg., Russia*

[□] *HPCAT, Carnegie Institution of Washington, Advanced Photon Source, ANL, Argonne, IL 60439, USA*

Submitted 5 Jule 2005

Magnetic behavior of a $Bi^{57}FeO_3$ powdered sample was studied at high pressures by the method of nuclear forward scattering (NFS) of synchrotron radiation. The NFS spectra from ^{57}Fe nuclei were recorded at room temperature under high pressures up to 61.4 GPa created in a diamond anvil cell. In the pressure interval $0 < P < 47$ GPa, the magnetic hyperfine field H^{Fe} at the ^{57}Fe nuclei increased reaching a value of ~ 52.5 T at 30 GPa, and then it slightly decreased to ~ 49.6 T at $P = 47$ GPa. As the pressure was increased further, the field H^{Fe} has abruptly dropped to zero testifying a transition from the antiferromagnetic to a nonmagnetic state (magnetic collapse). In the pressure interval $47 < P < 61.4$ GPa, the value of H^{Fe} remained zero. The field H^{Fe} has recovered to low-pressure values during decompression.

PACS: 71.27.+a, 71.30.+h, 81.40.Vw, 81.40.Tv

Introduction. The bismuth ferrite $BiFeO_3$ belongs to a class of ferromagnetoelectric materials (multiferroics) which have both a spontaneous electrical polarization and a spontaneous magnetization [1, 2]. Due to a record high antiferromagnetic Neel temperature ($T_N = 643$ K) and the ferroelectric's Curie temperature ($T_C = 1083$ K) between multiferroics [3, 4], the $BiFeO_3$ crystal is most attractive from both fundamental and applied aspects of science. It has the rhombohedrally distorted perovskite structure with space group $R3c$, and the unit cell parameters in the hexagonal representation are $a = 5.58$ and $c = 13.9$ Å (or $a_r = 3.96$ Å and $\alpha_r = 0.6°$ in the rhombohedral setting) [5,6].

In a local atomic scale, $BiFeO_3$ has the G-type antiferromagnetic structure, in which each iron ion has six iron neighbors with opposite spin directions [7]. However, the antiferromagnetic order is not homogeneous and a complex spatially modulated cycloid spin structure is present with a long wavelength of about 620 Å which is incommensurate with the crystal lattice [8 – 11].

As it was shown by Zvezdin and Pyatakov [1], the crystal symmetry of $BiFeO_3$ allows the existence of a linear magnetoelectric effect, spontaneous magnetization, and a toroidal moment. However, due to a spatially modulated spin structure, these effects average to zero over the crystal volume, and they can be observed only when the spatially modulated structure is destroyed [1]. Several mechanisms could suppress the modulated structure, and one of them is a strong applied magnetic field. The measurements in pulsed and static magnetic fields revealed an appearance of all three effects at the critical field of about 180–200 kOe when modulated spin structure is transformed to a uniform state [12 – 14]. The substitution of rare-earth ions for bismuth ions in $BiFeO_3$ can also destroy (suppress) the spin modulation and magnetoelectric effect appears [15].

In the present study, external high pressures were applied to the $BiFeO_3$ crystal to modify its magnetic properties. The method of resonant nuclear forward scattering (NFS) of synchrotron radiation at ^{57}Fe nuclei was used to investigate parameters of magnetic hyperfine interactions.

The experiment. High-quality $BiFeO_3$ powder samples in which iron was enriched with ^{57}Fe isotope to 98% were prepared. For high-pressure studies, a plate of $BiFeO_3$ was made by pre-compression of initial powder between diamond anvils. The thickness of the plate was about 5–10 microns. In an optical microscope, the plate was transparent of deep red color. To perform the NFS studies at high-pressures, the $Bi^{57}FeO_3$ plate with the dimensions $\sim 90 \times 90\ \mu m^2$ was placed into a high-pressure cell with diamond anvils. Diameter of the working surface of diamonds in the cell was about 300 μm and the diameter of the hole in the rhenium gas-

[1)] e-mail: lyubutin@ns.crys ras.ru

ket where the sample was placed was about 100 μm. To create a quasi-hydrostatic pressure, the working volume of the cell was filled with the polyethyl-siloxane liquid PES-5. The pressure value was determined by the standard ruby fluorescence technique. Several ruby chips with dimensions of about 1 μm were placed into the cell along with the sample. They were placed at different distances from the center of the working volume to evaluate the pressure gradient in the chamber.

The NFS experiments were performed at 16-ID-D beamline at Advanced Photon Source, Argonne National Laboratory. The time spectra of NFS from the ^{57}Fe nuclei (which may be considered as the *time-domain* Mössbauer spectra [16]) were recorded at room temperature in the pressure range up to $P = 61.4$ GPa during compression and decompression runs. A high-resolution monochromator with 2.2 meV bandwidth was tuned to nuclear resonance energy of 14.4125 keV of the Mossbauer transition in ^{57}Fe [17]. The polarization vector of gamma rays was horizontal and parallel to the sample plane.

Fig.1 presents the scattered radiation intensity versus time that elapsed after the nuclear excitation by an incident pulse. The measurements for different pressure values were performed in the 24 bunches mode of operation. These bunches were evenly distributed with 154 ns separation between them. The damped decay of nuclear excitation is modulated in time by quantum and dynamic beats. The quantum beats are caused by the interference of the scattered radiation components with different frequencies as a result of the nuclear level splitting into sublevels due to the hyperfine interaction. The period of quantum beats is inversely proportional to the hyperfine splitting and, in the case under study, to the magnetic field H^{Fe} at the iron nuclei. The dynamic beats are caused by multiple scattering processes and are determined by the sample thickness. A detailed description of the method can be found in a review [18].

Under pressures below 47 GPa, the main feature of the spectra is pronounced quantum beats. The spectra indicate that, over the whole pressure range from ambient pressure to 47 GPa, the period of beats slightly decreases indicating an increase of the magnetic hyperfine field H^{Fe} under pressure. When pressure increase above 47 GPa the high frequency quantum beats disappear signaling the disappearance of the magnetic field H^{Fe} at the ^{57}Fe nuclei (Fig.1). At decompression from the maximum pressure 61.4 GPa to below 47 GPa high frequency quantum beats have appeared again indicating reversibility of the magnetic transition. At ambient pressure the value of the field H^{Fe} calculated from the NFS spectra is 49.3 T, which is consistent with that

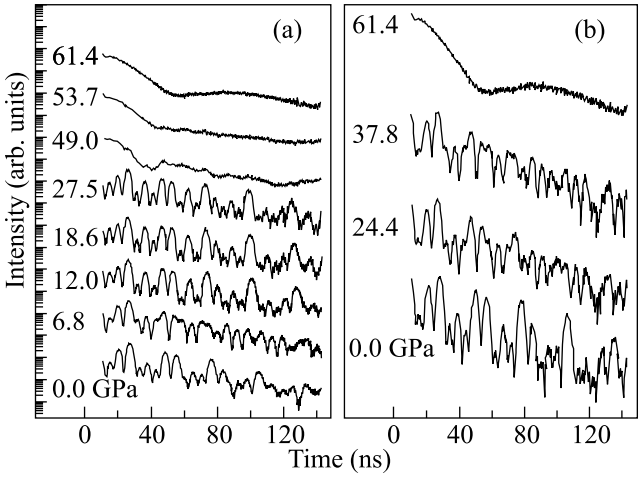

Fig.1. Evolution of NFS time spectra in the $Bi^{57}FeO_3$ powder sample with pressure increase (a) and pressure decrease (b) runs. The spectra are recorded at room temperature without applying an external magnetic field

obtained from previous Mössbauer [19, 20] and NMR [21, 10] experiments.

We also recorded the ^{57}Fe-Mossbauer absorption spectrum of our $Bi^{57}FeO_3$ sample in transmission geometry (Fig.2). At room temperature, the six-line spectrum

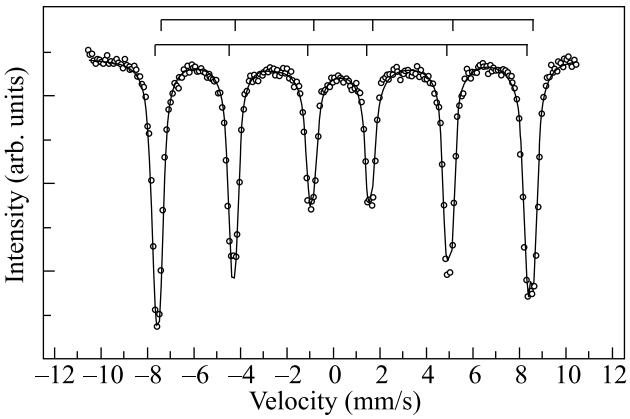

Fig.2. The ^{57}Fe-Mossbauer absorption spectrum of the $Bi^{57}FeO_3$ powder sample recorded at room temperature in transmission geometry. Symbols are the experimental points. The resulting fit to two subspectra is shown by solid line

has slightly broadened resonance lines with a noticeable asymmetry of first and sixth lines. As it was suggested by Zalesskii et al. [21] from analysis of the NMR data, such features of the spectrum may appear due to a distribution of values of the magnetic hyperfine fields at iron nuclei. In the spatially modulated cycloid spin structure of the $BiFeO_3$ crystal the magnetic moments of Fe ions are turning in the plane perpendicular to the hexago-

nal plane along the propagation direction of the spin-modulated wave (c-axis). Due to a variation of the dipole contribution to the magnetic hyperfine field H^{Fe} this field becomes a periodical function of a coordinate in the crystal lattice, with two maxima corresponding to the spin alignments parallel $H_{\|}$ and perpendicular $H_{\perp}$ to the crystal c-axis [10]. Taken into account these ideas, we fit successfully the Mossbauer spectrum (Fig.2) to two six-line components and obtained the following parameters: $H_{\|}^{Fe} = 49.96\,(8)$ T, and $H_{\perp}^{Fe} = 49.73\,(8)$ T.

Results and discussion. The NFS spectra were processed by the MOTIF program, developed by Shvyd'ko [22, 23]. The large number of quantum beats in each spectrum (more than 20) allows us to obtain the value of the magnetic field H^{Fe} at ^{57}Fe nuclei with high accuracy. The field H^{Fe}, being the main parameter of this study, practically does not correlate with other parameters of the spectrum such as the sample thickness, the quadrupole hyperfine splitting, and azimuthal orientation of the iron magnetic moment. All these parameters may affect only the relative heights of individual peaks of the high frequency quantum beats.

The room-temperature pressure dependence of the magnetic hyperfine field H^{Fe} is shown in Fig.3. The

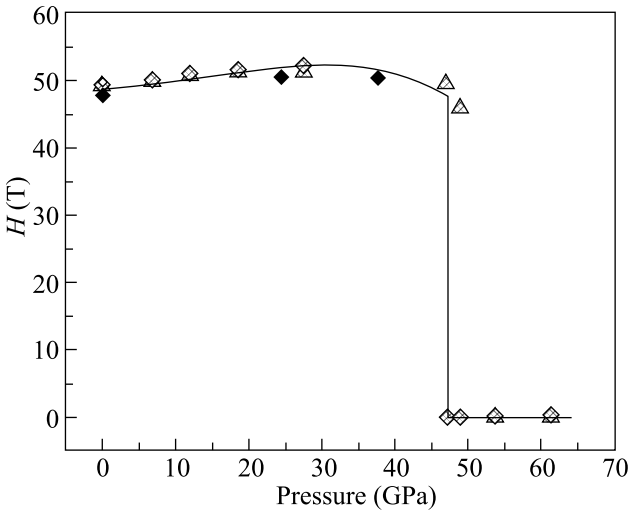

Fig.3. Pressure dependence of the magnetic hyperfine field at ^{57}Fe nuclei in $Bi^{57}FeO_3$ for the pressure increase (grey triangles and diamonds) and pressure decrease (black triangles) regimes. Solid line is a guide for the eye. The value of H^{Fe} from the Mossbauer absorption spectrum at normal conditions is represented by white diamond symbol

field increases from ~ 49.3 T at ambient pressure to a maximum value of ~ 52.5 T at $P \sim 30$ GPa, and then it slightly decrease to about 49.6 T at further pressure increase. At $P \sim 47$ GPa the magnetic field drops to zero, pointing to an abrupt transition of the sample from the magnetically ordered to a nonmagnetic state. Viewing control in an optical microscope revealed that after this transition the sample, been deep red in color at ambient pressure, darkens and becomes opaque. Presumably, this effect is due to a drastic decrease in the optical gap and may imply a transition from insulating to a metallic state.

It follows from Fig.3 that the increase in the magnetic field with pressure up to 30 GPa is almost linear. The pressure dependence of the field can be given as $H^{Fe} = H_0^{Fe} + k_H \cdot P$ with the parameters $H_0^{Fe} = 49.5 \pm 0.2$ T and $k_H = 0.09 \pm 0.01$ T/GPa. Apparently, the magnetic field increase with pressure is due to the increase in the exchange interaction as a result of enhancing of covalent bonding owing to the decrease in the Fe–O–Fe inter-ionic distances. A nonlinear behavior of the field with further pressure increase to 47 GPa is under question and may be related to some transformation in crystal structure or/and possibly electronic and magnetic transitions.

The most important effect is the abrupt disappearance of the magnetic field at the iron nuclei at $P \sim$ ~ 47 GPa. This effect occurs due to the transition of the $BiFeO_3$ crystal to a nonmagnetic state, demonstrating the collapse of localized magnetic moment of iron. Several mechanisms for explaining such a magnetic collapse can be proposed.

(1) A structural phase transition resulting in the formation of a new $BiFeO_3$ phase with the Neel point T_N below the room temperature. In this case, the magnetic transition at $P = 47$ GPa is a transition from antiferromagnetic to a paramagnetic insulating state.

(2) An insulator-to-metal transition at which the $3d$ electrons of Fe^{3+} ions are delocalized and form a conduction band. In this case, the magnetic state of the material is determined by the band mechanism and depends on the band structure. Then, the magnetic transition at $P = 47$ GPa can be a transition from antiferromagnetic to a paramagnetic metallic state.

(3) A transition of the iron ions from the high-spin to the low-spin state, analogous to the phenomenon that was recently observed in several complex iron oxides in the pressure range of 30–50 GPa [24–27]. As it follows from the Mossbauer spectra parameters (Fig.2), the trivalent iron ions in $BiFeO_3$ are in the high-spin state $S = 5/2$ at normal pressure. The low-spin state $S = 1/2$ of Fe^{3+} ions is not diamagnetic, but the Neel point T_N of such a material should be much lower than for materials with Fe^{3+} ions in the high-spin state. For example, in the mean-field approximation, it follows from the ratio $k_B \cdot T_N \propto A \cdot J \cdot S \cdot (S+1)$, where J is an exchange integral, k_B is the Bolzman's parameter, and A is a constant. In this case, the observed magnetic transition is

a transition from the high-spin antiferromagnetic to the low-spin paramagnetic state.

The measurements of nuclear isomer shifts (IS) and quadruple splitting (QS) would give direct information about the iron spin states [28]. In our study of the NFS spectra we did not intend to measure the IS and QS parameters, which would require a more sophisticated experimental technique. However, the IS and QS values can be reasonably obtained from the conventional Mossbauer absorption spectroscopy at high pressures, which we are going to fulfill in nearest future. An additional information about ions spin states can be obtained from the high resolution X-ray emission spectroscopy technique which is now available with synchrotron radiation facilities (description of this method could be seeing elsewhere [29]). These types of experiments, as well as the high-pressure X-ray diffraction studies of the $BiFeO_3$ crystal structure, are in our nearest plan.

We are grateful to Prof. A. A. Bush for preparation of the $BiFeO_3$ compound enriched with Fe-57 isotope and to Dr. K. V. Frolov for help in the Mossbauer absorption measurements. This work is supported by the DOE grant # DE-FG02-02ER45955, by the Russian Foundation for Basic Research grants # 04-02-16945-a and # 05-02-16142-a, and by the Program of Physical Branch of the Russian Academy of Sciences under the Project "Strongly correlated electronic systems". HP-CAT is a collaboration among the Carnegie Institution, Lawrence Livermore National Laboratory, the University of Hawaii, the University of Nevada Las Vegas, and the Carnegie/DOE Alliance Center (CDAC), and supported by DOE-BES, DOE-NNSA, NSF, DOD - TACOM, and the W.M. Keck Foundation. The use of the Advanced Photon Source is supported by the U.S. Department of Energy, Basic Energy Sciences, Office of Science, under Contract # W-31-109-EN.

1. A. K. Zvezdin and A. P. Pyatakov, Physics-Uspekhi **47**(4), 8 (2004).
2. G. A. Smolenskii and I. Chupis, Sov. Phys. Usp. **25**, 475 (1982).
3. G. A. Smolenskii, V. Yudin, E. Sher et al., Sov. Phys. JETP **16**, 622 (1963).
4. Yu. N. Venevtsev, G. Zhdanov, and S. Solov'ev, Sov. Phys. Crystallogr. **4**, 538 (1960).
5. P. Fischer, M. Polomskya, I. Sosnowska et al., J. Phys. C **13**, 1931 (1980).
6. J. D. Bucci, B. K. Robertson, and W. J. James, J. Appl. Crystallogr. **5**, 187 (1972).
7. S. V. Kiselev, R. P. Ozerov, and G. S. Zhdanov, Sov. Phys. Dokl. **7**, 742 (1963).
8. I. Sosnowska, T. Peterlin-Neumaier, and E. Steichele, J. Phys. C **15**, 4835 (1982).
9. I. Sosnowska, M. Loewenhaupt, W. I. F. David et al., Physica B **180-181**, 117 (1992).
10. A. V. Zalesskii, JETP **95**, 101 (2002).
11. J. Wang, J. Neaton, and H. Zheng, Science **299**, 1719 (2003).
12. Yu. F. Popov, Ferroelectrics **162**, 135 (1994).
13. Yu. F. Popov, A. M. Kadomtseva, S. Krotov et al., Low Temt. Phys. **27**, 478 (2001).
14. B. Ruette, Phys. Rev. B **69**, 064114 (2004).
15. A. M. Kadomtseva, Physica B **211**, 327 (1995).
16. R. Ruffer and A. I. Chumakov, Hyperfine Interact. **97/98**, 589 (1996).
17. Yu. V. Shvyd'ko, M. Lerche, J. Jäschke et al., Phys. Rev. Lett. **85**, 495 (2000).
18. G. V. Smirnov, Hyperfine Interact. **123/124**, 31 (1999).
19. C. Blaauw and F. van der Woude, J. Phys. C **6**, 1422 (1973).
20. De Sitter, Solid State Commun. **18**, 645 (1976).
21. A. V. Zalesskii, A. K. Zvezdin, A. A. Frolov, and A. A. Bush, JETP Lett. **71**, 465 (2000).
22. Yu. V. Shvyd'ko, Phys. Rev. B **59**, 9132 (1999).
23. Yu. V. Shvyd'ko, Hyperfine Interact. **125**, 173 (2000).
24. A. G. Gavriliuk, I. A. Trojan, I. S. Lyubutin et al., JETP **100**, 688 (2005).
25. A. G. Gavriliuk, I. A. Trojan, S. G. Ovchinnikov et al., JETP **99**, 566 (2004).
26. A. G. Gavriliuk, S. A. Kharlamova, I. S. Lyubutin et al., JETP Lett. **80**, 426 (2004).
27. A. G. Gavriliuk, I. A. Troyan, R. Boehler et al., JETP Lett. **77**, 619 (2003).
28. V. A. Sarkisyan, I. A. Troyan, I. S. Lyubutin et al., JETP Lett. **76**, 664 (2002).
29. J. Badro, G. Fiquet, V. V. Struzhkin et al., Phys. Rev. Lett. **89**, 205504 (2002).